THE JOURNAL OF PHYSICAL CHEMISTRY B

Article

pubs.acs.org/JPCB

Design and Synthesis of FRET-Mediated Multicolor and Photoswitchable Fluorescent Polymer Nanoparticles with Tunable Emission Properties

Jian Chen,*[,†,‡] Peisheng Zhang,[†] Gang Fang,[§] Pinggui Yi,*[,†] Fang Zeng,[§] and Shuizhu Wu[§]

[†]Key Laboratory of Theoretical Chemistry and Molecular Simulation of Ministry of Education, Hunan Province College Key Laboratory of QSAR/QSPR, School of Chemistry and Chemical Engineering, Hunan University of Science and Technology, 411201 China

[‡]Key Laboratory of Advanced Functional Polymeric Materials, Xiangtan University, 411105 China

[§]College of Materials Science & Engineering, South China University of Technology, 510640 China

Supporting Information

ABSTRACT: Novel multicolor and photoswitchcable fluorescent polymer nanoparticles were prepared by one-step miniemulsion via methyl methacrylate (MMA) copolymerization with 4-ethoxy-9-allyl-1,8-naphthalimide (EANI), allyl-(7-nitrobenzo[1,2,5]oxadiazol-4-yl)-amine (NBDAA) and spiropyran-linked methacrylate (SPMA). Under visible-light conditions, SPMA moieties in polymer nanoparticles are colorless and nonfluorescent, by varying the incorporating ratio of two dyes (EANI and NBDAA), fluorescence resonance energy transfer (FRET)-mediated emission signatures can be tuned so that the nanoparticles exhibit multiple colors under a single wavelength excitation. Moreover, the fluorescence emission of EANI and NBDAA dyes in nanoparticles can be reversibly switched "on" and "off" through the FRET process by the alternating irradiation of UV and visible light. This class of novel photoswitchable multicolor fluorescent polymer nanoparticles may find potential applications in multiplexed bioanalysis.

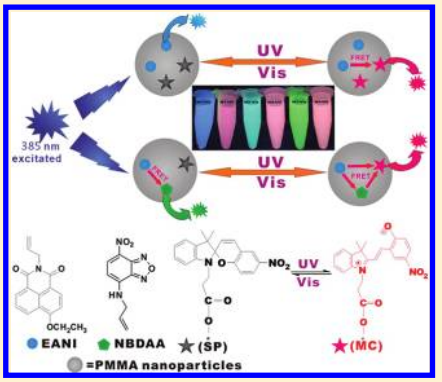

INTRODUCTION

In recent years, extensive attention has been paid to fluorescent materials due to their application potential in imaging,[1−3] labeling,[4,5] sensors,[6,7] etc. Multicolor fluorescent nanomaterials which exhibit multi distinguishable emission signals under a single wavelength excitation are especially attractive, due to they can minimize the complexity of fluorescent measurement, thereby remarkably simplifying the instrumentation requirements, and meanwhile allowing a simultaneous excitation of all fluorophores involved in the assay.[8−11] The popular strategy toward multiplexed emission focuses on the use of quantum dots (QDs), which provide a controllable emission and wide absorption bands.[12,13] However, Application of QDs as probes for fast scanning imaging and in vivo application is hampered by their "blink", cytotoxicity and incompatibility within aqueous media.[13,14] A promising solution to these problems, we suppose, is to incorporate two or more energy level-matched fluorescent dyes into nanoparticles to construct the nanoparticle-based FRET systems.[15−19] By varying the ratio of the two or three dyes, these fluorescent nanoparticles exhibit multicolor as well as distinguishable emission signals under single wavelength excitation. The additional benefits of these multicolor fluorescent nanoparticles reveal extraordinary high brightness, excellent stability and biocompatibility. Thus, a large number of encoding multicolor fluorescent nanoparticles population can be readily produced from a limited number of individual fluorophores.[16−18]

Covalently incorporating dyes into nanoparticles rather than dye-doping have attracted more attention, since it greatly reduced potential problems such as dye aggregation as well as leakage of dye from the particles,[17−26] which significantly improved the structural stability of the whole FRET system. For example, Wang and co-workers prepared fluorescent monodisperse polystyrene microspheres via covalently labeling with two energy levels well-matched dyes. By varying the dye concentrations, microspheres show tuned colors with different fluorescent intensity under a single wavelength excitation.[17] Tan et al. synthesized novel FRET-mediated silica nanoparticles, which exhibit multiple colors, as well as distinguishable emission signatures of the three tandem dyes under one single wavelength excitation.[18] Mecking et al. employed Glaser coupling polymerization as a suitable step-growth reaction to directly prepare multicolor fluorescent conjugated polymer nanoparticles in aqueous miniemulsion.[20]

The application of FRET-mediated multicolor fluorescent nanoparticles in multiplexed bioanalysis, such as simultaneous detection of multiple cancer cells, are highly promising for

Received: November 16, 2011
Revised: February 27, 2012
Published: March 20, 2012

   dx.doi.org/10.1021/jp2110659 | J. Phys. Chem. B 2012, 116, 4354−4362

potential applications in the sensitive monitoring of multiple cancer cells for biomedical research and medical diagnostics.[10] However, the extensible application of these multicolor nanoparticles using in vivo detection will be hindered by a lack of effective difference from false positive signals generated by adventitious fluorescent biomolecules.[27] To address this problem, a popular strategy is fabrication of FRET-mediated photoswitchable fluorescent systems which can provide the photoswitchable dual-color fluorescence states by modulating the state of the photochromic acceptor with cycles of UV−visible irradiation, allowing greatly increased signal detection by suppression of background signals.[22−26,28−30]

Herein, to extend the present FRET-mediated multicolor fluorescent nanoparticle systems and generate photoswitchable colors, in this work, we fabricated novel multicolor and photoswitchable fluorescent polymer nanoparticles by covalently incorporating three polymerizable fluorescent dyes, 4-ethoxy-9-allyl-1,8-naphthalimide (EANI), allyl-(7-nitro-benzo-[1,2,5]oxadiazol-4-yl)-amine (NBDAA), and spiropyran-linked methacrylate (SPMA), into the polymer nanoparticles via a facile one-step miniemulsion polymerization. The as-prepared novel multicolor and photoswitchable fluorescent polymer nanoparticles show high dye load, a controllable amount and ratio of the three dyes, and higher photostability because of covalent linkage between dye molecules and the particle. Under visible-light environment, the presence of SPMA in polymer nanoparticles exists in the colorless spiropyran form (SP form), and by varying the incorporating ratio of two dyes (EANI and NBDAA), FRET-mediated emission signatures can be adjusted to have the nanoparticles exhibit different colors under a single wavelength excitation. Moreover, UV and visible light can be applied to reversibly modulate the fluorescence emission of both EANI and NBDAA dyes in nanoparticles. Upon UV light irradiation, the spiropyran moieties in nanoparticles are converted to the (merocyanine) MC form and upon visible-light irradiation they return to the SP form; thus, the fluorescence emission of both EANI and NBDAA dyes can be reversibly switched between on and off (Scheme 1). Overall, this class of novel multicolor and photoswitchable fluorescent polymer nanoparticles will be favorable for high-resolution multiplexed bioassays.

Scheme 1. Schematic Illustration of Novel Multicolor and Photoswitchable Fluorescent Polymeric Nanoparticles Covalently Incorporating Two (EANI and SPMA) or Three Fluorescent Dyes (EANI, NBDAA, and SPMA) under Excitation at 385 nm

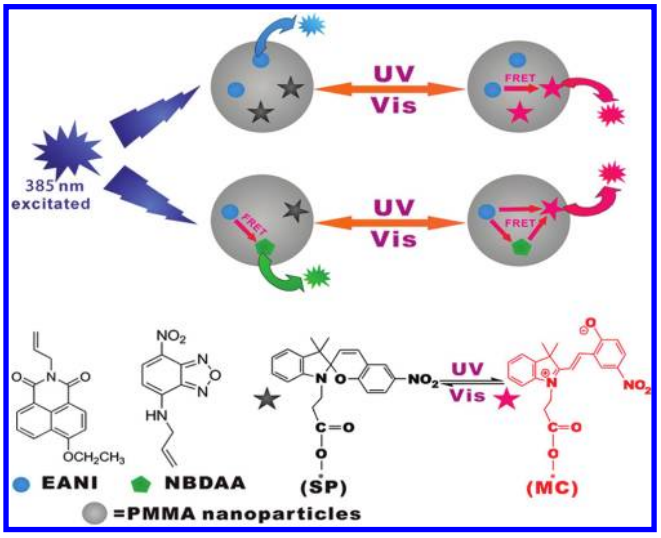

EXPERIMENTAL SECTION

Materials. The surfactant sodium dodecyl sulfate (SDS, 99%, Aldrich), *n*-hexadecane (HD, 99%, Aldrich), 4-bromo-1,8-naphthalic anhydride (99%, TCI), 4-chloro-7-nitrobenzofurazan (NBD-Cl, 99%, TCI), allylamine (99%, Aladdin), *N,N′*-dicyclohexylcarboiimide (DCC, 99%, Alfa), and 4-dimethylamino-pyridine (DMAP, 99%, Alfa) were used as received. Dichloromethane (A.R.) was washed with sulfuric acid and then distilled from CaH_2. 2-Hydroxyethyl methacrylate (HEMA, 97%, Aldrich) was dissolved in water (25 vol %) and washed four times with an equal volume of hexane and then dried over MgSO4 and distilled under vacuum prior to use. Potassium persulfate (KPS, 99.99%, Aldrich) was recrystallized from water and dried under vacuum. Methyl methacrylate (MMA, Aldrich) was purified by distillation under vacuum to remove inhibitors. The water used in this work is the double-distilled water which was further purified with a Milli-Q system. Tetrahydrofuran (THF, A.R.) and Triethylamine (A.R.) were distilled over CaH_2. Petroleum ether, benzene, and other reagents were analytical reagents and used without further purification.

Synthesis of 4-Ethoxy-9-allyl-1,8-naphthalimide (EANI) Monomer. EANI was synthesized according to modified literature procedures.[31] First, 4-bromo-n-substituted-l,8-naphthalimides was prepared according to literature procedures.[32] Typical procedures are as follows. A mixture of 9.6 g of (0.03 mol) 4-bromo-*N*-allylnaphthalimide and 1.8 g of KOH was dissolved in 150 mL of ethanol. The solution was refluxed. After 4 h the liquor was poured into 600 mL of water, and the resulting crystals were filtered and dried in vacuum (95% yield). ^{1}H NMR spectrum for the product is shown in Figure S1 (500 MHz, $CDCl_3$, 25 °C) (ppm): 1.6 (3H, CH_3), 4.3 (2H, $-CH_2-$), 4.7 (2H, $-CH_2-$), 5.2 (2H, olefinic protons), 6.0 (1H olefinic protons), 6.7−8.6 (5H, aromatic protons).

Synthesis of Allyl-(7-nitro-benzo[1,2,5]oxadiazol-4-yl)-amine (NBDAA) Monomer. Allyl-(7-nitro-benzo[1,2,5]-oxadiazol-4-yl)-amine (NBDAA) was synthesized according to slightly modified literature procedures.[33] 4-Chloro-7-nitro-2,1,3-ben-zoxadiazole (NBD-Cl; 200 mg, 1.00 mmol) was dissolved in acetonitrile (40 mL). After the addition of allylamine (140 μL), the solution was stirred at room temperature for 30 min. The reaction mixture was evaporated to dryness under reduced pressure, and the residues were purified by silica gel column chromatography using CH_2Cl_2 as the eluent to afford NBDAA (70% yield). ^{1}H NMR spectrum for the product is shown in Figure S2 (500 MHz, $CDCl_3$, 25 °C) (ppm): 4.1 (2H, $-CH_2-$), 5.4 (2H, olefinic protons), 6.0 (1H, olefinic protons), 6.2 - 8.5 (2H, aromatic protons).

Synthesis of the Spiropyran-Linked Methacrylate (SPMA) Monomer. SPMA were synthesized with a slightly modified procedure reported elsewhere.[28] During the synthesis process, all of the reaction vessels were wrapped with aluminum foil, so as to ensure the reaction was performed in the dark. For the synthesis of SPMA, first l-(β-carboxyethyl)-3′,3′-dimethyl-6-nitrospiro(indoline-2′,2-chromane) (SPCOOH) was synthesized according to a literature procedure.[34] Subsequently, SPCOOH (3.8 g, 10 mmol), HEMA (5.2 g, 40 mmol), and DMAP (0.41 g, 3 mmol) were added to a 100 mL round-

dx.doi.org/10.1021/jp2110659 | J. Phys. Chem. B 2012, 116, 4354−4362

Table 1. List of Some Data of Two or Three Dye-Incorporated Nanoparticle Samples

	EANI [mg ($\times 10^{-4}$ M)]		NBDAA [mg ($\times 10^{-4}$ M)]		SPMA [mg ($\times 10^{-3}$ M)]		
sample[a]	feed	determined[b]	feed	determined[c]	feed	determined[d]	Dm[e] [nm]
NP-P1	0	0	0	0	0	0	78.9
NP-P2	2(6.0)	1.84(5.5)	0	0	0	0	83.4
NP-P3	0	0	1.2(4.6)	1.12(4.3)	0	0	84.2
NP-P4	0	0	0	0	5(0.85)	4.4(0.75)	79.5
NP-P5	2(6.0)	1.81(5.4)	1.2(4.6)	1.11(4.3)	0	0	82.3
NP-N1	2(6.0)	1.80(5.4)	0	0	5(0.85)	4.1(0.70)	85.6
NP-N2	2(6.0)	1.84(5.5)	0.3(1.1)	0.28(1.0)	5(0.85)	4.4(0.75)	81.5
NP-N3	2(6.0)	1.83(5.5)	0.6(2.3)	0.55(2.1)	5(0.85)	4.4(0.75)	80.6
NP-N4	2(6.0)	1.84(5.5)	0.9(3.4)	0.85(3.2)	5(0.85)	4.3(0.73)	83.6
NP-N5	2(6.0)	1.80(5.4)	1.2(4.6)	1.11(4.3)	5(0.85)	4.4(0.75)	80.2

[a]The MMA/HD/SDS/KPS feed is 0.625/0.038/0.025/0.022 g, respectively. [b]Calculated by using the absorbance of EANI at 366 nm in nanoparticle dispersion (eliminate the effect of scattering light) and the molar extinction coefficient of EANI in dichloromethane, (ε = 13 000 mol^{-1} L cm^{-1}); [c]Calculated by using the absorbance of NBDAA at 448 nm in nanoparticle dispersion (eliminate the effect of scattering light) and the molar extinction coefficient of NBDAA in dichloromethane, (ε = 19 000 mol^{-1} L cm^{-1}); [d]Calculated by using the absorbance of SPMA at 340 nm in nanoparticle dispersion (eliminate the effect of scattering light) and the molar extinction coefficient of SPMA in dichloromethane (ε = 8780 mol^{-1} L cm^{-1}); [e]Average nanoparticle diameter, determined from DLS data.

bottomed flask equipped with a pressure-equalized dropping funnel, magnetic stirrer, and nitrogen inlet. Cold dry THF (80 mL) was added to the flask, and the solution was cooled to 0 °C; a red brown solution resulted. DCC solution (2.06 g, 10 mmol in THF) was added to the resulted solution via the pressure-equalized dropping funnel over 60 min. The flask was maintained at 0 °C for 2 h, and then the temperature was raised gradually to room temperature over about 24 h. The product was filtrated with cold dry THF (3 × 40 mL) to give a red filtrate. After most of the solvent was removed under vacuum distillation, the residual was washed by a larger amount of distilled water to remove the unreacted HEMA. The precipitate was dissolved in benzene and filtrated again to remove the unreacted SPOOH. Afterward most of the solvent was evaporated under vacuum and below 45 °C to avoid SPMA polymerization, and the solution was precipitated in a large amount of petroleum ether. Finally a fine red purple precipitate of purified 2-(3-(3′,3′-dimethyl-6-nitrospiro(indoline-2′,2-chromane)-1′-yl)propanoyloxy)-ethyl-methacrylate (SPMA) was obtained. The target product was dried in a vacuum oven overnight at room temperature. The ^{1}H NMR spectrum of this product is shown in Figure S3 in the Supporting Information. ^{1}H NMR (500 MHz, $CDCl_3$, 25 °C) (ppm): 1.0−1.3 (CH_3 of spiropyran, 6H), 1.8−1.9 (CH_3 of HEMA, connected to olefinic carbon, 3H), 2.6−2.7 (−CH_2COO− of spiropyran, 2H), 3.5−3.6 (−CH_2N- of spiropyran, 2H), 4.2 (−CH_2O− of HEMA, 4H), 5.5−6.0 (olefinic protons, CH_2 and two CH, 4H), 6.6−8.1 (aromatic protons).

Preparation of Novel Multicolor and Photoswitchable Fluorescent Polymerization Nanoparticles. A mixture containing the monomers and hydrophobes (MMA, EANI, NBDAA, SPMA, and HD) was added to a water solution with emulsifier (SDS) and stirred (1000 r/min) for 15 min, and then the mixture was ultrasonicated for 20 min (KQ5200DE) to obtain a miniemulsion. The mixture was purified with Milli-Q cooled in an ice-bath during ultrasonication to avoid heating. The resulting miniemulsion was put into a 50 mL flask equipped with a condenser, which was immersed in an oil bath with a thermostat. The polymerization was started by adding an aqueous solution of KPS and preceded at 60 °C for 210 min. After the polymerization, the as-prepared nanoparticle dispersions were percolated, and finally the nanoparticles dispersions were obtained.

Sample Irradiation. Samples were irradiated using a UV hand-held lamp (300 nm, 2.8 mW/cm^2) and green LED lamp (525 ± 5 nm, 1.34 mW/cm^2). Samples were placed in 10 × 10 mm quartz cuvettes, filled such that the entire sample was exposed to light, thereby eliminating mixing effects.

Characterization. ^{1}H NMR spectra were recorded on a Bruker Avance 500 MHz NMR spectrometer. The nanoparticle diameters were determined by a Malvern Nano-ZS90 instrument, and their morphology was observed with an atomic force microscope (AFM, Seiko SII 400) in the tapping mode. UV−vis spectra were recorded on a Shimadzu UV-2501PC spectrophotometer at room temperature. Fluorescence spectra were recorded on a Shimadzu RF-5301PC fluorescence spectrophotometer at room temperature. The cyclic voltammetric measurements were carried out with a CH Instruments 631A apparatus. Ag/Ag$^+$ was used as the reference electrode, a glassy carbon as the working electrode, and a Pt wire as the auxiliary electrode. The redox potentials were measured in argon bubbled acetonitrile using 0.1 M tetrabutylammonium hexafluorophosphate (Bu_4NPF_6) as the supporting electrolyte. The scanning speed was maintained at 0.1 V/s.

RESULTS AND DISCUSSION

Preparation of Novel Multicolor and Photoswitchable Fluorescent Polymeric Nanoparticles. In this work, three chromophores (EANI, NBDAA, and SPMA) were chosen carefully to allow for efficient FRET: EANI was used as general donor for NBDAA and MC state of SPMA, whereas NBDAA acted as both an acceptor for EANI and a donor for MC state of SPMA. By using a facile one-step miniemulsion polymerization, one or two fluorescent dyes (EANI and NBDAA) and photochromic spiropyran derivative (SPMA) were covalently incorporated into nanoparticles to construct the nanoparticle-based multicolor and photoswitchable FRET systems. Obviously, this approach can effectively avoid the dye leakage, which is an undesired effect observed with nanoparticles as the dyes were noncovalently incorporated into the polymeric nanoparticles.[15] The prepared fluorescent nanoparticles display photoswitchable multicolor fluorescence under a single wavelength excitation by either varying EANI-NBDAA ratio or

dx.doi.org/10.1021/jp2110659 | J. Phys. Chem. B 2012, 116, 4354−4362

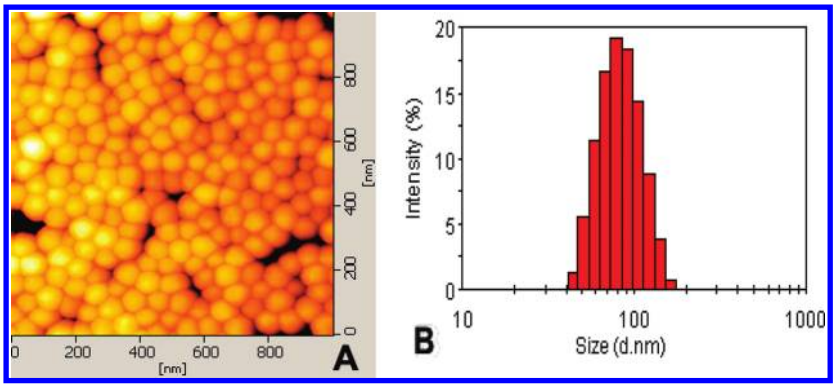

Figure 1. (A) AFM image of a fluorescent nanoparticle sample (sample NP-N5). (B) Size distribution for the nanoparticle sample NP-N5 determined by DLS.

alternately irradiating UV/visible light while fixing their ratio, as illustrated in Scheme 1.

By typical one-step miniemulsion polymerization, nanometer-sized particles with the average diameters of 80 nm were obtained by adjusting the amount of surfactant, monomer concentration in water, as well as the ultrasonification power and time,[15,35,36] as determined by dynamic light scattering (DLS, Table 1). Figure 1A shows an atomic force microscopy (AFM) image for a typical nanoparticle sample (NP-N5). It can be seen that most of the polymer particles of the sample were discrete and regular with diameters ranging from 75 to 85 nm. Its stable dispersion with an average diameter of 80.2 nm and narrow size distribution is determined by DLS (Figure 1B). The above results demonstrate that the miniemulsion polymerization is a promising method to fabricate uniform polymer nanoparticles with defined size.

Spectroscopic Properties of Multicolor and Photoswitchable Fluorescent Nanoparticles and Study of the Energy Fransfer between Donor and Acceptor within the Nanoparticle. Figure 2 depicts the absorption spectra of a photoswitchable nanoparticle sample (NP-N5) and spiropyran-contained nanoparticle dispersion (NP-P4). It is well-known that spiropyran can assume one of two stable states: the open-ring state, known as merocyanine (MC) state, and the closed-ring state, known as spiro (SP) state (Scheme 1).[28,37] As shown in Figure 2, upon visible light irradiation, spiropyran moieties in the nanoparticles assumed the SP state and exhibited no absorption from 500 to 700 nm (NP-N5 upon vis); while with UV irradiation, a new absorption band at 500−700 nm appeared due to the formation of the MC state (NP-N5 upon UV), suggesting that spiropyran moieties have been successfully incorporated into nanoparticles, which is in good agreement with our previous report.[28] The EANI and NBDAA dyes exhibit very low absorption and weak fluorescence emission in saturated aqueous solution owing to their very low solubility in water (Figure S4). However, with the covalently incorporation of EANI and NBDAA dyes into the nanoparticles, two prominent absorption for EANI (λ = 366 nm) and NBDAA (λ = 448 nm) appear (NP-N5 upon Vis), which are close to that for EANI and NBDAA in dichloromethane, respectively (Figure S4A). Moreover, both the fluorescence intensity of the EANI and NBDAA dye-contained nanoparticles dispersion increased greatly compared to their saturated aqueous solution as they were located in a low-polarity circumstance (Figure S4B). The above results reveal that the EANI, NBDAA, and spiropyran derivate have been successfully incorporated into the nanoparticles and shielded from the external aqueous environment. The amount of the EANI, NBDAA, and spiropyran moieties in the nanoparticle dispersion are given in Table 1, which can be deduced by using the absorbance values assuming that the molar extinction coefficient of EANI, NBDAA, or spiropyran moieties in nanoparticles are the same as that in a certain organic solution (Figure S5).[15,28]

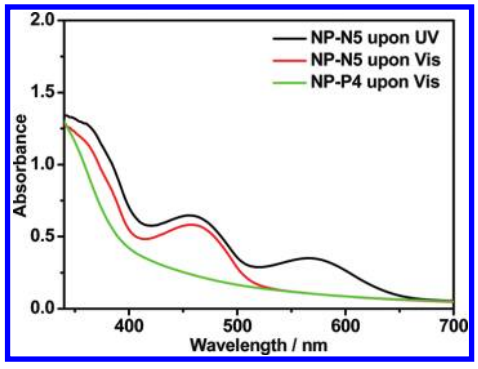

Figure 2. Absorption spectra of a fluorescent nanoparticle dispersion sample (NP-N5) and SPMA-contained nanoparticle dispersion (NP-P4).

For fluorescence modulation systems using the dyad or triad strategy, the emission behavior of the donor−acceptor pair (fluorophore−fluorophore, fluorophore−spiropyran, or other photochromes) can be adjusted by virtue of the photoinduced electron transfer (PET), FRET, or both of them.[38−43] The measured reduction potentials and the spectral data allow a quantitative estimation of the thermodynamic driving force for the PET process in terms of the free energy changes (ΔG). The ΔG values have been calculated using $\Delta G = E_{ox(D/D^+)} - E_{red(A^-/A)} - E_{0,0} - 0.06$,[39,41,43] where $E_{ox(D/D^+)}$ represents the oxidation potential for the EANI or NBDAA, respectively (Figure S6A and S6B). $E_{red(A^-/A)}$ represents the reduction potential of NBDAA or the MC state of SPMA, respectively (Figure S6C and S6D). $E_{0,0}$ denotes the energy of the first-excited singlet state of the fluorophore (EANI or NBDAA). The $E_{0,0}$ values used in the calculation of ΔG have been estimated from the location of the first peak position in the fluorescence spectrum.[41] The measured ΔG values of three donor−acceptor pairs (EANI-NBDAA, EANI-MC, and NBDAA-MC) in this system have been shown in Table S1 (see Supporting Information). As seen from Table S1, the ΔG values for PET for both EANI-MC and NBDAA-MC pair are positive, indicating that PET is thermodynamic impossible in

dx.doi.org/10.1021/jp2110659 | J. Phys. Chem. B 2012, 116, 4354−4362

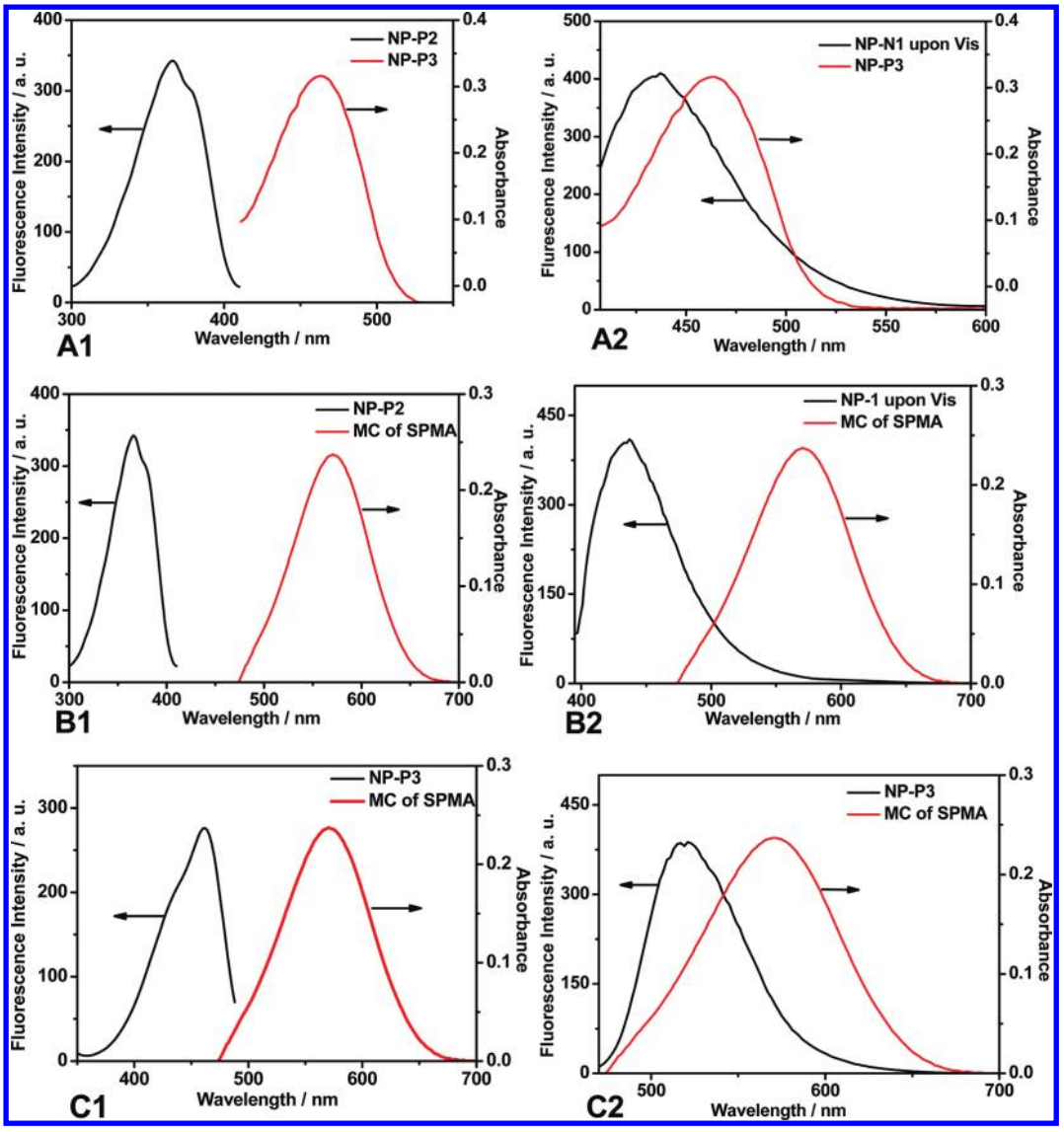

Figure 3. Fluorescence spectrum of donor (balck curve) and absorption spectrum of acceptor (red curve) in nanoparticles: (A1) EANI (excitation) and NBDAA (absorption), (A2) EANI (emission) and NBDAA (absorption); (B1) EANI (excitation) and MC state of SPMA moieties (absorption), (B2) EANI (emission) and MC state of SPMA moieties (absorption); (C1) NBDAA (excitation) and MC state of SPMA moieties (absorption), (C2) NBDAA (emission) and MC state of SPMA moieties (absorption).

these system. Presumably, the FRET from the excited EANI or NBDAA to the MC state of the spiropyran moiety is mainly responsible for the decrease in the emission intensity of this system. Nevertheless, as for the EANI-NBDAA pair, the ΔG value for PET is slight negative, suggesting that PET from the excited EANI to NBDAA is also responsible for the decrease in the emission intensity of the EANI. However, on the basis of previous work,[15] we have demonstrated that the FRET can be efficiently occurred from the donor (EANI) to acceptor (NBDAA) in a single nanoparticle (Figure S7). They are consistent with some reported results.[15,17,18] To simplify the complex model systems, Here, we mainly focus on the FRET between EANI and NBDAA.

Figure 3 displays a series of the corresponding spectra matching for the donor's fluorescence spectrum with the acceptor's absorption spectrum. Interestingly, seldom overlaps can be found between donor's fluorescence excitation spectrum and acceptor's absorption spectrum (Figure 3A1, Figure 3B1 and Figure 3C1). However, by way of comparison, the EANI fluorescence emission band not only fully matches the absorption band of NBDAA (Figure 3A2), but also generally matches the absorption band of MC state of SPMA moieties (Figure 3B2); and the NBDAA fluorescence emission band overlaps well with the absorption band of MC state of SPMA moieties (Figure 3C2). According to the principle of FRET,[43] for efficient FRET to take place, the FRET pair must exhibit significant overlap of the donor's emission spectrum with the acceptor's absorption spectrum, and the distance between the donor to the acceptor should be within the effective Förster radius (generally, 1 to 10 nm). For these fluorescence modulation systems, the distance between donor and acceptor can be controlled by inserting a suitable spacer between them or modulating their amount and ratio in size-defined nanoparticles.[25,28] Thus, they can be integrated into the polymer nanoparticles to fabricate efficient luminescent systems with FRET features. Moreover, from the perspective of an energy-level match, the energy of the first-excited singlet state of EANI was estimated to be 2.84 eV.[28] Similar calculations based upon

dx.doi.org/10.1021/jp2110659 | J. Phys. Chem. B 2012, 116, 4354–4362

absorption and emission maxima gave a first-excited singlet-state energy of 2.40 eV for the NBDAA, 3.65 eV for the SP form of the SPMA in nanoparticles, and 2.05 eV for the MC form of the SPMA.[28] These data also indicate that energy transfer from EANI or NBDAA to the SP form is impossible; whereas that from EANI to the NBDAA or MC form of SPMA, and from NBDAA to the MC form of SPMA are possible.

Figure 4A illustrates the fluorescence spectra of partial FRET-mediated samples. It can be seen from Figure 4A, under

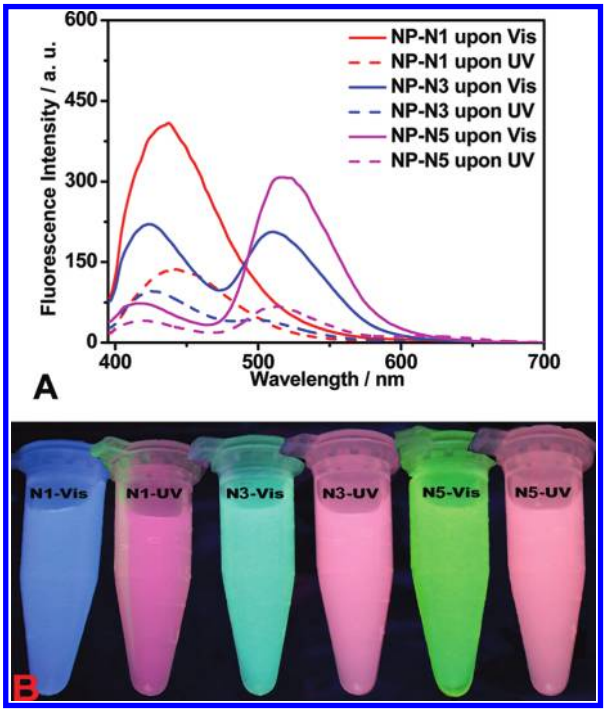

Figure 4. (A) Fluorescence emission spectra of three nanoparticle samples with different NBDAA feed (for samples NP-N1, NP-N3, and NP-N5, the NBDAA feed increased at a certain value) after visible light irradiation and UV irradiation; (B) photograph for three nanoparticles dispersion (NP-N1, NP-N3, and NP-N5) after visible light irradiation and UV irradiation under the dark environment.

visible-light conditions, that SPMA moieties in nanoparticles are colorless and nonfluorescent, by changing the ratio of EANI and NBDAA in nanoparticles, the fluorescence emission property of the nanoparticles dispersion can be correspondingly varied under single wavelength excitation (Figure 4A).[15,17,18] The above fluorescence emission changes can also be visualized by the naked eye, as evidenced from the transition from blue to green (Figure 4B). In agree with the previous studies.[15,17,18]

On the other hand, when these fluorescent nanoparticle dispersions were exposed to UV light (300 nm, 2.8 mW/cm^2), the characteristic fluorescence emissions for EANI and NBDAA (with different molar feed ratios) were mainly quenched and a weak emission band at 650 nm appeared (Figure S8B), which can be attributed to the MC form of spiropyran moieties; while after the irradiation of visible light (525 ± 5 nm, 1.34 mW/cm^2), the fluorescence intensity of EANI and NBDAA recovered (Figure 4A and Figure S8A), respectively, indicating that the observed quenching of both EANI and NBDAA fluorescence can be arose through energy transfer (FRET) from EANI and NBDAA dyes to the MC form of spiropyran moieties. In addition, the appearance of aqueous dispersion of fluorescent nanoparticles can also be reversibly modulated by UV and visible light irradiation (Figure 4B).

Unlike some FRET-based dyad systems in which donor and acceptor are connected by covalent bonds, the three fluorophores in the nanoparticles of the current work were segregated by the PMMA matrix. The distance between the donor and acceptor moieties within the nanoparticles is not a fixed value and cannot be accurately determined, and one donor can interact with multiple acceptors residing in close proximity simultaneously. According to the Förster non-radiative energy transfer theory,[43] the energy transfer efficiency E, expressed by eq 1, depends on the Förster critical radius R_0, the average number of acceptors interacting with the donor, and the distance (r) between the donor and the acceptor. The energy transfer is effective over distances in the R_0 = ±50% R_0 range.

$$E = \frac{{R_0}^6}{{R_0}^6 + r^6} \tag{1}$$

The magnitude of R_0 is dependent on the spectral properties of the donor and the acceptor molecules. If the wavelength λ is expressed in nanometers, then $J(\lambda)$ is in units of M^{-1} cm^{-1} nm^4 and the Förster critical radius, R_0 in angstroms (Å), is expressed as follows (eq 2):

$$R_0 = 0.2108[\kappa^2 \Phi_D n^{-4} J(\lambda)]^{1/6} \tag{2}$$

where K^2 is the orientation factor for the emission and absorption dipoles and its value depends on their relative orientation, n is the refractive index of the medium and Φ_D is the quantum yield of the donor. $J(\lambda)$ is the overlap integral of the fluorescence emission spectrum of the donor and the absorption spectrum of the acceptor (Figure 3, panels A2, B2, and C2) [eq 3].

$$J(\lambda) = \int_0^\infty F_D(\lambda)\varepsilon_A(\lambda)\lambda^4 \, d\lambda \tag{3}$$

where $F_D(\lambda)$ is the fluorescence intensity of the donor in the absence of acceptor, $\varepsilon_A(\lambda)$ is molar extinction coefficient of the acceptor, λ is wavelength. In the current experimental conditions, the Förster distances (R_0) of the three donor–acceptor pairs (EANI-NBDAA, EANI-MC, NBDAA-MC) in nanoparticles have been calculated. For instance, the Förster distances (R_0) between donor (EANI) and acceptor (NBDAA) has been calculated as 41.5 Å, assuming random orientation of the EANI and NBDAA taking K^2 = 2/3, n_R = 1.49 (PMMA), and Φ_D = 0.74[31] (Table 2). The other data are illustrated in Table 2.

We also calculated the average number of EANI (N_{EANI}/NP), NBDAA (N_{NBDAA}/NP) and spiropyran (N_{SP}/NP) in a nanoparticle (Table 3), the average ratio of NBDAA number to EANI number (N_{NBDAA}/N_{EANI}), spiropyran number to EANI number (N_{SP}/N_{EANI}) and spiropyran number to NBDAA

Table 2. Calculated R_0 of the Three Donor–Acceptor Pairs

donor	acceptor	Φ_D	$J(\lambda)$ (M^{-1} cm^{-1} nm^4)	R_0 (nm)	$D_{effective}$[a] (nm)
EANI	NBDAA	0.74	5.76×10^{14}	4.15	6.23
EANI	MC	0.74	1.34×10^{13}	2.22	3.33
NBDAA	MC	0.95	2.30×10^{14}	3.71	5.57

[a]Effective energy transfer distance (R_0 + 50% R_0).[43,44]

dx.doi.org/10.1021/jp2110659 | J. Phys. Chem. B 2012, 116, 4354–4362

Table 3. Characteristics of Five EANI, NBDAA, and Spiropyran-Containing Nanoparticle Samples

sample[a]	D_{NP}[b] [nm]	C_{EANI}[c] [× 10^{-4} M]	N_{EANI}/NP	C_{NBDAA}[c] [× 10^{-4} M]	N_{NBDAA}/NP	C_{SPMA}[c] [× 10^{-3} M]	N_{SP}/NP
NP-N1	85.6	5.4	2600			0.70	3333
NP-N2	81.5	5.5	2294	1.0	471	0.75	3176
NP-N3	80.6	5.5	2167	2.1	833	0.75	3000
NP-N4	83.6	5.5	2438	3.2	1438	0.73	3313
NP-N5	80.2	5.4	2053	4.3	1579	0.75	2842

[a]The MMA/HD/SDS/KPS feed is 0.625/0.038/0.025/0.022 g, respectively. [b]D_{NP}: average nanoparticle diameter, determined from DLS data; [c]C_{EANI}, C_{NBDAA}, and $C_{spiropyran}$: mole concentration of EANI, NBDAA, and spiropyran in dispersion respectively, determined from the absorbance values.

Table 4. Characteristics of the Three EANI, NBDAA, and Spiropyran-Contained Nanoparticle Samples

sample	N_{NBDAA}/N_{EANI}	N_{A1}[a]	E_1[b] [%]	r_1[c] [nm]	N_{SP}/N_{EANI}	N_{A2}[a]	E_2[b] [%]	r_2[c] [nm]	N_{SP}/N_{NBDAA}	N_{A3}[a]	E_3[b] [%]	r_3[c] [nm]
NP-N1					1.3	1.6	67.6	1.96				
NP-N2	0.2	1.7	27.9	4.86	1.4	1.4	60.6	2.07	6.7	8.1	85.7	2.75
NP-N3	0.4	3.1	53.0	4.07	1.4	1.7	54.5	2.15	3.6	7.9	83.5	2.83
NP-N4	0.6	4.8	70.9	3.58	1.4	1.7	46.5	2.27	2.3	7.8	81.3	2.90
NP-N5	0.8	5.9	86.4	3.05	1.4	1.6	41.5	2.35	1.8	7.6	78.4	2.99

[a]The number of NBDAA residing around one donor EANI (N_{A1}), spiropyran residing around one donor EANI (N_{A2}), spiropyran residing around one donor NBDAA (N_{A3}) within the effective energy transfer distance, respectively (see the Supporting Information). [b]The experimental energy transfer efficiency of three donor−acceptor pairs (EANI-NBDAA (E_1), EANI-MC (E_2), and NBDAA-MC (E_3); see the Supporting Information). [c]The estimated average distance of three donor−acceptor pairs (EANI-NBDAA (r_1), EANI-MC (r_2), and NBDAA-MC (r_3); see the Supporting Information).

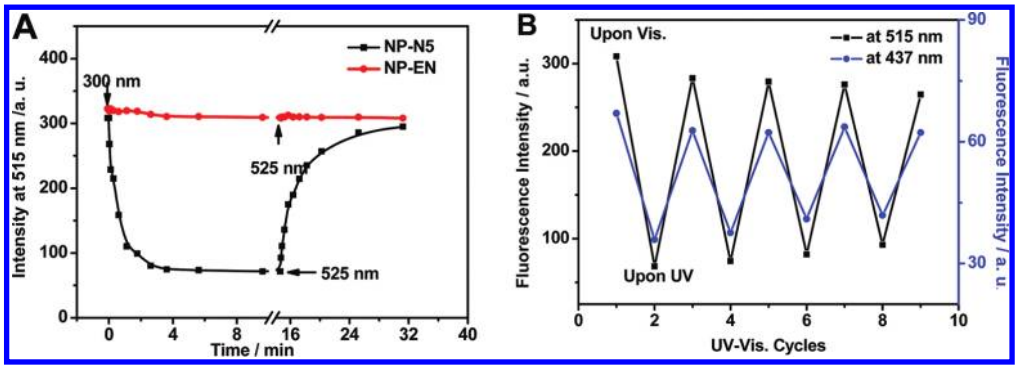

Figure 5. Fluorescence response (excitated at 385 nm and emitted at 515 nm) of sample NP-N5 on irradiation with 300 nm UV and then 525 nm visible light (A) and fluorescence intensity change at 437 and 515 nm for the nanoparticles sample NP-N5 after UV illumination and visible light irradiation cycles (B).

number (N_{SP}/N_{NBDAA}) in one nanoparticle, the experimental energy transfer efficiency (E_x) for the donor−acceptor pairs in the different nanoparticle samples as well as the estimated average distance between donor and acceptor in nanoparticles (r_x) for the different samples (Table 4). In addition, considering that the energy can be transferred from a donor to an acceptor if their separation distance is less than the upper limit of efficient energy transfer (1.5 R_0). We also estimated the number of the acceptor (N_{Ax}) residing around one donor within the effective energy transfer distance, assuming that the dispersion of spiropyran molecules, NBDAA or EANI molecules in the whole nanoparticle is homogeneous, and the existence of the donor does not affect the dispersion of the acceptor and vice versa, The data (N_{Ax}) are given in Table 4.

As seen from Table 4, for the five nanoparticle samples from NP-N1 to NP-N5, in most of the samples there are multiple acceptors around a donor within the effective energy transfer distance, and this ensures the intraparticle FRET process to take place from donor to acceptor. Under visible-light conditions, SPMA moieties in polymer nanoparticles are colorless and nonfluorescent; the energy transfer from EANI (donor) to NBDAA (acceptor) effectively occurrs, for instance, as for the nanoparticle sample with a highest ratio of NBDAA to EANI (NP-N5); there are more NBDAA molecules around a EANI (donor) molecule (5.9); and higher experimental energy transfer efficiency can be achieved (86.4%). However, for the sample with the lowest ratio of NBDAA to EANI (NP-N1), on average, there are only 1.7 effective acceptors (NBDAA) around an EANI within effective energy transfer distance, and the experimental energy transfer efficiency is 27.9%. With the irradiation of UV light, the energy transfer from EANI (donor) to the MC form of spiropyran (acceptor) and from NBDAA (donor) to the MC form of spiropyran (acceptor) can take place because of the transformation of spiropyran moieties from the SP form to the MC form. It is clearly evident that the energy transfer efficiency (E_2) of the donor−acceptor pair (EANI-MC) within nanoparticles from NP-N1 to NP-N5 gradually decreased upon the gradual increasing of NBDAA feed. The occurrence of this phenomenon was due to the overlap efficiency of the donor's emission spectrum (EANI) with the acceptor's absorption spectrum (NBDAA) exhibited significantly better than that of another donor−acceptor pair

dx.doi.org/10.1021/jp2110659 | J. Phys. Chem. B 2012, 116, 4354−4362

(EANI-MC), and the FRET process between EANI and NBDAA can more effectively occur. In addition, with the gradual increasing of the NBDAA feed, the average number of spiropyran (N_A) residing around one donor (NBDAA) within the effective energy transfer distance decreased (see N_{SP}/N_{NBDAA} in Table 4); thus, E_3 of donor−acceptor pair (NBDAA-MC) within nanoparticles from NP-N1 to NP-N5 gradually diminished (see E_3 in Table 4). The above results indicate that the control of the acceptor to donor ratio during the polymerization is important for obtaining nanoparticle dispersion with well-defined energy transfer efficiency as well as fluorescence emission property.

Photoreversible Modulation (Switching) of Fluorescence of Multicolor Nanoparticle Dispersion. Figure 5 shows typical photoresponsive behavior as well as the reversible nature of the aqueous dispersion of nanoparticle dispersions (NP-N5) upon exposure to alternating cycles of UV (300 nm) and visible light (525 nm) illumination. It can be seen from Figure 5A that the change in fluorescence intensity of EANI-NBDAA containing nanoparticles dispersion (NP-P5) at 515 nm are not apparent, thus, its photodegradation is neglectable in such short-time irradiation by low energy UV (2.8 mW/cm^2) or visible light (1.34 mW/cm^2). However, as for the sample NP-N5, upon irradiation with 300 nm light, most of the fluorescence intensity at 515 nm gradually decreased over 10 min and then the dispersion recovered its fluorescence intensity upon 20 min of visible light irradiation. Moreover, Figure 5B also indicated that the fluorescence of NBDAA at 515 nm can be reversibly switched "on" and "off" upon irradiation with UV and visible light. The light-induced switching of fluorescence can be repeated several times with only a slight fatigue effect. In addition, the change in fluorescence intensity of this sample at 437 nm is also displaying relatively fast photoresponsivity (Figure S9) and fairly good photoreversibility upon alternate UV/vis irradiation.

CONCLUSION

In summary, we have fabricated nanoparticle-based photoswitchable multicolor fluorescent systems by covalently incorporating three chromophores (EANI, NBDAA, and SPMA) into the polymer nanoparticles via one-step miniemulsion polymerization and demonstrated that the fluorescence emission signatures of EANI and NBDAA dyes can be tuned to have the nanoparticles exhibit multiple colors under a single wavelength excitation by either varying their ratios or irradiating upon UV/visible light through reversible light-induced structural transformation of SPMA moieties while fixing their ratios. This class of novel multicolor photoswitchable fluorescent polymer nanoparticles may find potential applications in multiplexed bioimaging and bioanalysis.

ASSOCIATED CONTENT

Supporting Information

^{1}H NMR spectra of EANI, NBDAA, and SPMA monomers. Detailed description of the calculation of the fluorescence quantum yield of the donor NBDAA, experimental energy transfer efficiency and estimation of donor−acceptor distance, and estimation of N_A (number of acceptors residing around one donor within the effective energy transfer distance). This material is available free of charge via the Internet at http://pubs.acs.org.

AUTHOR INFORMATION

Corresponding Author

*E-mail: cj0066@gmail.com; pgyi@hnust.cn.

Notes

The authors declare no competing financial interest.

ACKNOWLEDGMENTS

This work was supported by NSFC (Project Nos. 51003026, 50973032, 21172066, and 21025415), Hunan Provincial Natural Science Foundation of China (No.11JJ4016), and the Open Project Program of Key Laboratory of Advanced Functional Polymeric Materials (Xiangtan University), College of Hunan Province (No. AFPM200907).

REFERENCES

(1) Day, R. N.; Davidson, M. W. *Chem. Soc. Rev.* **2009**, *38*, 2887−2921.
(2) Andresen, M.; Stiel, A. C.; Fölling, J.; Wenzel, D.; Schönle, A.; Egner, A.; Eggeling, C.; Hell, S. W.; Jakobs, S. *Nat. Biotechnol.* **2008**, *26*, 1035−1040.
(3) Wu, C.; Szymanski, C.; Cain, Z.; McNeill, J. *J. Am. Chem. Soc.* **2007**, *129*, 12904−12905.
(4) Bittermann, H.; Siegemund, D.; Malinovskii, V. L.; Haner, R. *J. Am. Chem. Soc.* **2008**, *130*, 15285−15287.
(5) Komatsu, T.; Kikuchi, K.; Takakusa, H.; Hanaoka, K.; Ueno, T.; Kamiya, M.; Urano, Y.; Nagano, T. *J. Am. Chem. Soc.* **2006**, *128*, 15946−15947.
(6) Dave, N.; Chan, M. Y.; Huang, P. J. J.; Smith, B. D.; Liu, J. W. *J. Am. Chem. Soc.* **2010**, *132*, 12668−12673.
(7) Wada, A.; Tamaru, S.; Ikeda, M.; Hamachi, I. *J. Am. Chem. Soc.* **2009**, *131*, 5321−5330.
(8) An, B. K.; Gihm, S. H.; Chung, J. W.; Park, C. R.; Kwon, S. K.; Park, S. Y. *J. Am. Chem. Soc.* **2009**, *131*, 3950−3957.
(9) Li, Z. Q.; Zhang, Y.; Jiang, S. *Adv. Mater.* **2008**, *20*, 4765−4769.
(10) Chen, X. L.; Estevez, M. C.; Zhu, Z.; Huang, Y. F.; Chen, Y.; Wang, L.; Tan, W. H. *Anal. Chem.* **2009**, *81*, 7009−7014.
(11) Wu, C.; Bull, B.; Szymanski, C.; Christensen, K.; McNeill, J. *ACS Nano* **2008**, *2*, 2415−2423.
(12) Han, M. Y.; Gao, X. H.; Su, J. Z.; Nie, S. *Nat. Biotechnol.* **2001**, *19*, 631−635.
(13) Michalet, X.; Pinaud, F. F.; Bentolila, L. A.; Tsay, J. M.; Doose, S.; Li, J. J.; Sundaresan, G.; Wu, A. M.; Gambhir, S. S.; Weiss, S. *Science* **2005**, *307*, 538−544.
(14) Derfus, A. M.; Chan, W. C. W.; Bhatia, S. N. *Nano Lett.* **2004**, *4*, 11−18.
(15) Chen, J.; Zhang, P. S.; Yi, P. G. *J. Macromol. Sci., Part A: Pure Appl. Chem.* **2010**, *47*, 1135−1141.
(16) Gaughan, R. *Photonics Spectra* **2006**, *40*, 121−122.
(17) Wu, W. B.; Wang, M. L.; Sun, Y. M.; Huang, W.; Cui, Y. P.; Xu, C. X. *Opt. Mater.* **2008**, *30*, 1803−1809.
(18) Wang, L.; Tan, W. H. *Nano Lett.* **2006**, *6*, 84−88.
(19) Xu, J. Q.; Liang, J. L.; Li, J.; Yang, W. S. *Langmuir* **2010**, *26*, 15722−15725.
(20) Baier, M. C.; Huber, J.; Mecking, S. *J. Am. Chem. Soc.* **2009**, *131*, 14267−14273.
(21) Pecher, J.; Huber, J.; Winterhalder, M.; Zumbusch, A.; Mecking, S. *Biomacromolecules* **2010**, *11*, 2776−2780.
(22) Davis, C. M.; Childress, E. S.; Harbron, E. J. *J. Phys. Chem. C* **2011**, *115*, 19065−19073.
(23) Harbron, E. J.; Davis, C. M.; Campbell, J. K.; Allred, R. M.; Kovary, M. T.; Economou, N. J. *J. Phys. Chem. C* **2009**, *113*, 13707−13714.
(24) Harbron, E. J. *Photochemistry*; RSC Publishing: London, 2011; Vol. *39*, pp 211−227.
(25) Zhu, L. Y.; Wu, W. W.; Zhu, M. Q.; Han, J. J.; Hurst, J. K.; Li, A. D. Q. *J. Am. Chem. Soc.* **2007**, *129*, 3524−3526.

(26) Fölling, J.; Polyakova, S.; Belov, V.; van Blaaderen, A.; Bossi, M. L.; Hell, S. W. *Small* **2008**, *4*, 134−142.
(27) Chudakov, D. M.; Verkhusha, V. V.; Staroverov, D. B.; Souslova, E. A.; Lukyanov, S.; Lukyanov, K. A. *Nat. Biotechnol.* **2004**, *22*, 1435−1439. Ando, R.; Mizuno, H.; Miyawaki, A. *Science* **2004**, *306*, 1370−1373.
(28) Chen, J.; Zhang, P. S.; Fang, G.; Yi, P. G.; Yu, X. Y.; Li, X. F.; Zeng, F.; Wu, S. Z. *J. Phys. Chem. B* **2011**, *115*, 3354−3362.
(29) Li, C. H.; Zhang, Y. X.; Hu, J. M.; Cheng, J. J.; Liu, S. Y. *Angew. Chem., Int. Ed.* **2010**, *49*, 5120−5124.
(30) Wu, T.; Zou, G.; Hu, J.; Liu, S. *Chem. Mater.* **2009**, *21*, 3788−3798.
(31) Grabchev, I.; Konstantinova, T. *Dyes. Pigm.* **1997**, *33*, 197−203.
(32) Konstantinova, T. N.; Meallier, P.; Grabchev, I. *Dyes. Pigm.* **1993**, *22*, 191−198.
(33) Onoda, M.; Uchiyama, S.; Santa, T.; Imai, K. *Anal. Chem.* **2002**, *74*, 4089−4096.
(34) Fissi, A.; Pieroni, O.; Ruggeri, G.; Ciardelli, F. *Macromolecules* **1995**, *28*, 302−309.
(35) Landfester, K. *Colloid Chem. II* **2003**, *227*, 75−123.
(36) Landfester, K. *Angew. Chem., Int. Ed.* **2009**, *48*, 4488−4507.
(37) Wu, S. Z.; Luo, Y. L.; Zeng, F.; Chen, J.; Chen, Y. N.; Tong, Z. *Angew. Chem., Int. Ed.* **2007**, *46*, 7015−7018.
(38) Bahr, J. L.; Kodis, G.; de la Garza, L.; Lin, S.; Moore, A. L.; Moore, T. A.; Gust, D. *J. Am. Chem. Soc.* **2001**, *123*, 7124−7133.
(39) Tomasulo, M.; Deniz, E.; Alvarado, R. J.; Raymo, F. M. *J. Phys. Chem. C* **2008**, *112*, 8038−8045.
(40) Chen, J.; Zeng, F.; Wu, S. Z. *Chemphyschem* **2010**, *11*, 1036−1043.
(41) Ramachandram, B.; Saroja, G.; Sankaran, N. B.; Samanta, A. *J. Phys. Chem. B* **2000**, *104*, 11824−11832.
(42) Sariciftci, N. S.; Smilowitz, L.; Heeger, A. J.; Wudl, F. *Science* **1992**, *258*, 1474−1476.
(43) Lakowicz, J. R. *Principles of fluorescence spectroscopy*; Springer: New York, 2006.
(44) Frigoli, M.; Ouadahi, K.; Larpent, C. *Chem.—Eur. J.* **2009**, *15*, 8319−8330.